

# THE GALAXY HALO FORMATION IN THE ABSENCE OF VIOLENT RELAXATION AND A UNIVERSAL DENSITY PROFILE OF THE HALO CENTER.

A. N. BAUSHEV

DESY, 15738 Zeuthen, Germany and  
Institut für Physik und Astronomie, Universität Potsdam, 14476 Potsdam-Golm, Germany

*Draft version June 13, 2018*

## ABSTRACT

While N-body simulations testify for a cuspy profile of the central region of the dark matter haloes, observations favor a shallow, cored density profile of the central region of, at least, some spiral galaxies and dwarf spheroidals. We show that a central profile, very close to the observed one, inevitably forms in the center of dark matter haloes if we make a supposition about a moderate energy relaxation of the system during the halo formation. If we assume the energy exchange between dark matter particles during the halo collapse to be not too intensive, the profile is universal: it depends almost not at all on the properties of the initial perturbation and is very akin, but not identical, to the Einasto profile with small Einasto index  $n \sim 0.5$ . We estimate the size of the 'central core' of the distribution, i.e., the extent of the very central region with a respectively gentle profile, and show that the cusp formation is unlikely, even if the dark matter is cold. The obtained profile is in a good agreement with observational data for, at least, some types of galaxies, but clearly disagrees with N-body simulations.

*Subject headings:* Astroparticle physics – cosmology: dark matter – elementary particles – cosmology: large-scale structure of universe

## 1. INTRODUCTION

The problem of the Universe structure formation is still far from the complete solution. Since the task is essentially nonlinear, N-body simulation is one of the possible ways to solve it. While their results satisfactorily describe observed properties of galaxy clusters (Okabe et al. 2010), some discrepancy seems to appear when we consider galaxy haloes. N-body simulations predict a very steep, NFW-like density profile of the central region of the dark matter haloes (Navarro et al. 1997). The Navarro-Frenk-White profile behaves there as  $\rho \propto r^{-1}$ . Though recent simulations favour the Einasto profile (Moore et al. 1998; Gao et al. 2008; Diemand et al. 2008; Stadel et al. 2009; Navarro et al. 2010)

$$\rho = \rho_s \exp \left[ -2n \left\{ \left( \frac{r}{r_s} \right)^{\frac{1}{n}} - 1 \right\} \right] \quad (1)$$

with a finite density in the center (Einasto 1965), the index of the profile is so high (typically,  $n \simeq 5 - 6$ ) that it can also be considered as a cuspy one.

On the contrary, observations (de Blok et al. 2001; de Blok & Bosma 2002; Marchesini et al. 2002; Gentile et al. 2007) show that galaxies have a core (i.e. a region with rather a shallow density profile) in the center. Chemin et al. (2011) fitted the dark matter density profiles of a large array of spiral galaxies by the Einasto profile, considering the Einasto index  $n$  as a free parameter. They found that Einasto profile provides a significantly better fit of observational data of the central region than either NFW or the cored pseudo-isothermal profiles. However, the Einasto index is found to be small ( $n \simeq 0.5 - 1$ ), that actually corresponds to a cored profile and is not in agreement with the predictions from  $\Lambda$ CDM simulations. Dwarf galaxies also show no cusps

in their centra (Oh et al. 2011; Governato et al. 2012).

There are several possible ways to account for this disagreement. It can be caused by the influence of baryon matter (Pontzen & Governato 2012). However, this explanation is not doubtless. The fraction of baryons in some dwarf galaxies is so tiny that it hardly can influence the cusp formation (Garrison-Kimmel et al. 2013), but these objects show no cusps in their centra. Meanwhile, galaxy clusters have a much larger fraction of baryons, and their density profiles are rather steep (Okabe et al. 2010). The problem of the baryon influence on the dark matter distribution is very complex and yet not quite clear. It lies beyond the scope of the present work, and we will not discuss it in this paper anymore, addressing the readers to the vast literature on this topic (see (Weinberg et al. 2013; Pontzen & Governato 2014) and references therein). The absence of the cusps could be a sign that the dark matter is warm and consists of light particles like sterile neutrinos. Thus the 'cusp vs. core' problem might shed light upon the physical nature of dark matter. However, we should first be sure that there is no explanation to the cores in the framework of cold DM paradigm.

We will try to show by this paper that the energy evolution of the forming halo is probably the key to the problem of central cusp occurrence. Though the density shape in the center of the halo may differ from the NFW profile, we will use the NFW halo concentration  $c_{vir}$  to qualitatively characterize a halo, because of popularity of the NFW profile. Let us denote by  $\epsilon = \frac{v^2}{2} + \phi$  the total energy of a unit mass of the matter,  $\phi$  is the gravitational potential. It is easy to show (see the beginning of section 2) that in the very general case the particles that later form the halo have very narrow initial energy distribution: the initial energies of the particles differ no more than 2 times. When a halo collapses, remarkable inhomogeneities and caustics appear; their strong small-

scale gravitational field mediates a relaxation and may significantly smear out the energy spectrum of the dark matter particles with respect to the initial one. A question appears: how strong can the relaxation be, i.e., can the energy evolution of the system be arbitrarily strong, or the ratio between the final  $\epsilon_f$  and the initial  $\epsilon_i$  energies is somehow limited for the majority of the particles?

In principle, the ratio  $\epsilon_f/\epsilon_i$  could be arbitrarily large: the idea of the 'violent relaxation' (Lynden-Bell 1967) was the supposition that a particle completely forgets its initial state during the relaxation, and its final energy has no connection with the initial one. However, the equilibrium solution obtained by Lynden-Bell (1967) has infinite total mass, and its applicability to the finite systems is discussible. The main fraction of mass of the future halo is initially concentrated in the outer layers with the highest initial  $r$  (since their volume grows as  $r^2$ ). Meanwhile, as it was shown by Lynden-Bell (1967), the efficiency of all relaxation processes (and so the alternation of the particle energy) rapidly drops with  $r$ : even in that work the outer part of the system remained unrelaxed. Moreover, simulations show that a significant part of the total mass of the halo accretes to the already collapsed halo (Wang et al. 2012). This substance has a respectively high total energy and cannot be significantly affected by the violent relaxation.

Unfortunately, the halo collapse is a very complex nonlinear process, and there is almost no hope to find an exact theoretical solution of the problem. The literature offers several possible approaches to the task. Syer & White (1998) suggested that the cuspy DM haloes might arise as a consequence of hierarchical structure formation. However, this theory predicts very steep cusps ( $\rho \propto r^{-2}$ ) in the case of Zeldovich-Harrison spectrum of initial perturbations. This cusp shape is hardly comparable with modern observations and simulations, while Planck Collaboration et al. (2013) firmly confirms the Zeldovich-Harrison spectrum. An another approach is to introduce Boltzmann's H-function (Tremaine et al. 1986; Stiavelli & Bertin 1987) that is actually the entropy of the system. The system cannot reach the real maximum of entropy, which is the isothermal sphere, but the authors suggest that the H-function increasing defines the direction of the system evolution. However, Pontzen & Governato (2013) correctly pointed to the possible difficulties of this approach. The violent relaxation (whatever violent it is) is actually a collisionless relaxation through the common field. This process is, in principle, reversible, and the entropy does not grow in it (Landau & Lifshitz 1980; Pontzen & Governato 2013). A good illustration for this statement is the existence of stationary solutions, like Osipkov (1979) or Jaffe (1983). These systems are very far from the entropy maximum, in particular, the local velocity distribution there is not Maxwell. However, they cannot relax anymore, since their gravitational field is already stationary. The only process that guarantees the entropy growth is the particle collisions. The characteristic of the collisional relaxation is (Binney & Tremaine 2008, eqn. 1.38)

$$\tau_r = \frac{N(r)}{8 \ln \Lambda} \tau_d \quad (2)$$

where  $v$ ,  $N(r)$ ,  $\ln \Lambda$ , and  $\tau_d = r/v$  are the 'characteris-

tic' particle velocity, the number of particles inside radius  $r$ , the Coulomb logarithm, and the dynamical time of the system at  $r$ , respectively. The dynamical time of the galaxies is typically only a few orders of magnitude smaller than the age of the Universe. Since a galactic halo may contain  $\sim 10^{65}$  particles (accepting the DM particle mass 200 GeV), the relaxation time enormously exceeds the age of the galaxies. So the entropy growth can be completely negligible at the cosmological time. Moreover, the system can hardly be ergodic in this case, which is necessary to use the statistical methods (Pontzen & Governato 2013). Surely, the statistically stable state is the isothermal sphere, i.e. it is cuspy. However, the applicability of the essentially statistical approach to a system that has existed for only a tiny fraction of the true relaxation time is discussible.

N-body simulations give a more direct way to investigate the halo relaxation. The idea of the method is to substitute real tiny DM particles by massive test bodies with smoothed Newtonian potential. Recent N-body simulations (Diemand et al. 2005, 2007; Diemand & Kuhlen 2008) indicate that the supposition of violent relaxation is not true: the energies of the majority of the particles do not change completely and correlate with the initial ones. Nevertheless, the relaxation is rather strong, and the halo profiles are cuspy.

The method has a weak point, however: the number of the test bodies is small as compared with the real DM particles, and the influence of the unphysical test body collisions should be carefully avoided. According to (2), the relaxation time is proportional to  $N(r)$ . The closer we approach the halo center, the smaller the number of the bodies  $N(r)$  is. At some radius  $r_{conv}$  the ratio of the simulation time  $t_0$  to the relaxation time  $\tau_r$  may go so large that the collisions become important. So the simulations are still reliable outside the convergence radius  $r_{conv}$ , but the density profile is already corrupted by the unphysical test body collisions inside  $r_{conv}$ .

As we have already mentioned, the dark matter in simulations rather rapidly forms stationary haloes with an almost universal density profile. The profile is close to the NFW, being cuspy ( $\rho \propto r^{-\gamma}$ ,  $\gamma \simeq 1$ ) or very steep in the center. The persist appearance of the cusp and its stability with respect to parameter variations of N-body codes is usually considered as a proof of its physical nature and independence on the collisions. The commonly-used method (Navarro et al. 2010) to assure the negligibility of the collisions is to find the moment when the the cusp starts to smear out, which is believed to be the first sign of the collision influence (Power et al. 2003). However, the cusp turns out to be surprisingly stable. Power et al. (2003) found that the smearing does not appear at least up to  $t = 1.7\tau_r$  and probably much longer. Indeed, Hayashi et al. (2003); Klypin et al. (2013) observed that the cusp was stable even at tens of relaxation times, and only then smeared out. The negligibility of the test body collisions at  $t \sim 30\tau_r$  seems suspicious. In order to test the influence of the particle encounters analytically the Fokker-Planck equation was used (Evans & Collett 1997; Baushev 2013c). It turned out that the density distribution close to NFW ( $\rho \propto r^{-\gamma}$ ,  $\gamma \simeq 1$ ) is an attractor solution for the kinetic equation, taking into account close encounters. The Fokker-Planck diffusion occurring as a result of the collisions transforms

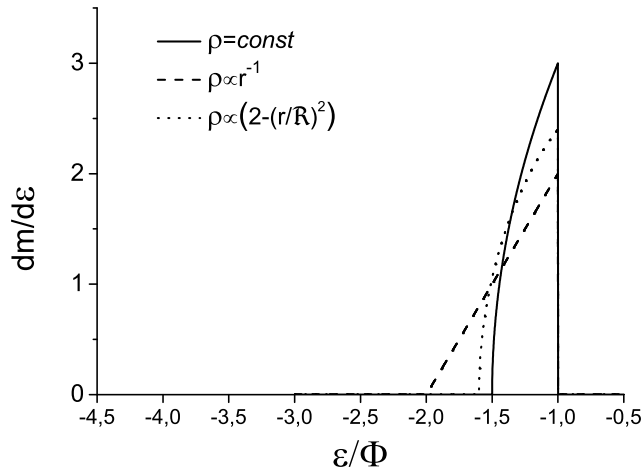


FIG. 1.— Energy spectra  $\frac{dm}{d\varepsilon}$  for various forms of initial perturbations. Apparently, there are no particles with  $\varepsilon > -\Phi$ .

any initial density distribution shallower than  $\rho \propto r^{-1}$  into a NFW-like profile ( $\gamma \simeq 1$ ) in a time  $t < \tau_r$ . Being formed, the cuspy profile should survive for a much longer time interval, since the collision effects are self-compensated to a first approximation in this case. Moreover, since the shape of the attractor solution is not sensitive to the simulation parameters, the cusp should be insensitive as well. At tens of relaxation times  $\tau_r$  the NFW-like profile should be smeared out by the ‘thermal conductivity’, which is a second-order effect of particle collisions (Quinlan 1996; Baushev 2013c).

These results perfectly describe the simulation behavior. The cusp forms at  $t < \tau_r$ , survives for several or even many relaxation times, and then smears out in tens relaxation times. However, since the test body collisions are unphysical and correspond to nothing real, the cusp formation by the Fokker-Planck diffusion is a purely numerical effect. As we could see, the collisions of real DM particles are completely ineffective. Thus the commonly-used criterion of the convergence radius  $r_{conv}$  of simulations  $t < 1.7\tau_r$  (Power et al. 2003) seems excessively optimistic. The fact that the cusp is stable and insensitive to the simulation parameters is not enough to state that the profile is not affected by the unphysical collisions. The only reliable criterion is  $t \ll \tau_r$ . However, it claims much more test bodies inside  $r_{conv}$  and so increases several times the convergence radius. This can be of vital importance for the ‘cusp vs. core’ problem. Actually, the disagreement between the simulations and observations occur only quite close (a few percent of  $R_{vir}$ ) to the halo center. If we use the more reliable criterion  $t \ll \tau_r$ , the contradictions may disappear.

The main aim of this paper is to show that a cored profile, very similar to that observed in the centra of the galaxies, inevitably forms in the center of dark matter haloes if we make the only supposition that the energy relaxation of the galactic dark matter haloes was *moderate* in the following sense:

*The principle assumption.* For the majority of the particles, the final energy in the formed halo  $\varepsilon_f$  differs no more than  $c_{vir}/3$  times from the initial value  $\varepsilon_i$

$$\frac{\varepsilon_f}{\varepsilon_i} \leq \frac{c_{vir}}{3} \quad (3)$$

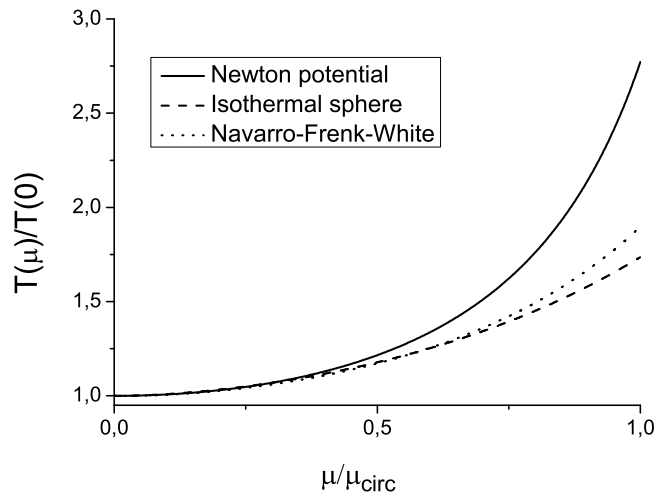


FIG. 2.— Ratios  $T(\mu)/T(0)$  for the newtonian potential  $\phi \propto -1/r$  (solid line), isothermal sphere  $\phi \propto \ln(r)$  (dashed line) and Navarro-Frenk-White profile with  $c_{vir} = 5$  (dotted line). The normalization of the potentials is chosen so that the mass inside  $r_0$  is the same for all three cases.  $\mu_{circ}$  corresponds to the circular orbit.

Concentration  $c_{vir}$  of the Milky Way galaxy lies between 12 and 17 (Klypin et al. 2002), and should be even higher for smaller galaxies (Navarro et al. 2010). So the moderate relaxation supposition means that the energies of the majority of the particles have not changed more than 4-5 times for the Milky Way galaxy; for less massive haloes the assumption is even softer. Of course, there are always particles, which energies have changed more than (3); however, we suppose that their fraction is small. The condition of the moderate relaxation will be specified and restated in the Discussion section.

We should underline that we suggest the moderate relaxation only for relatively low-mass objects like haloes of galaxies. Moreover, despite of all the reasoning above, this is no more than a hypothesis: now the assumption cannot be certainly proved, while the validity of all results of this article depends on the feasibility of this basic supposition. However, as we will see, the fulfilment of condition (3) automatically leads to a central density profile in good agreement with observations. For this reason alone it is worthy to consider the moderate relaxation, at least as a hypothesis.

## 2. ENERGY SPECTRUM

Let us consider the initial distribution of matter. Hereafter in this article we will consider a spherically-symmetric task and neglect the presence of baryon matter. The mass and initial radius of the halo are  $m$  and  $\mathfrak{R}$ ,  $\mathfrak{R} \simeq R_{vir}$ . If the dark matter is cold, the initial velocity of the matter may be thought of as to be zero without loss of generality (Gorbunov & Rubakov 2011). (As we will see at the end, the conclusions of this section is also valid for the warm dark matter). To begin with, let us consider the case when the matter is uniformly distributed inside  $\mathfrak{R}$  ( $\rho = const$ , the Tolman case). Inside the sphere:

$$\phi(r) = \frac{Gm}{\mathfrak{R}} \left( \frac{1}{2} \left( \frac{r}{\mathfrak{R}} \right)^2 - \frac{3}{2} \right) \quad (4)$$

$$dm = 3 \frac{m}{\mathfrak{R}} \left( \frac{r}{\mathfrak{R}} \right)^2 dr \quad (5)$$

Hence we obtain the initial energy distribution of the substance:

$$\frac{dm}{d\epsilon} = \left( \frac{3\mathfrak{R}}{G} \right) \sqrt{3 + \frac{2\epsilon}{\Phi}}; \quad \epsilon \in \left[ -\frac{3}{2}\Phi; -\Phi \right] \quad (6)$$

where  $\Phi \equiv \frac{Gm}{R_{vir}} \simeq \frac{Gm}{\mathfrak{R}}$ . Performing similar calculations, we obtain for the case of initial density perturbation  $\rho \propto r^{-1}$

$$\frac{dm}{d\epsilon} = \frac{2m}{\Phi} \left( 2 + \frac{\epsilon}{\Phi} \right); \quad \epsilon \in [-2\Phi; -\Phi] \quad (7)$$

As one can see in Fig. 1, distributions (6) and (7) differ not so strongly: all the particles lie in a respectively narrow energy range  $[-2\Phi; -\Phi]$  and the majority of the particles have energies close to  $-\Phi$ . Moreover, the initial energy spectrum of any real (smooth) density perturbation lies between (6) and (7): the perturbation collapses when  $\frac{\delta\rho}{\rho} = \beta \simeq 1$ , and  $\beta$  weakly depends on its shape.

Consequently, if the initial shape of  $\delta\rho(r)$  is a smooth function, distributions of  $\phi$  and  $dm$  differs from (4) and (5) only on a multiplier of the order of 2. As a result, distribution  $dm/d\epsilon$  does not differ very significantly from the uniform one (6). As an illustration, we also consider profile  $\rho \propto (2 - (r/\mathfrak{R})^2)$  that well approximates real initial perturbations. The corresponding energy distribution, represented in in Fig. 1, turns out to be quite close to (6).

It seems reasonable to say that the initial energy distribution is similar to (6) under any reasonable choice of shape of the initial perturbations. If we divide a spherically symmetric initial distribution on radial layers of thickness  $dr$ ,  $\epsilon$  is constant within the layer, and the volume of the layer grows as  $(\frac{r}{\mathfrak{R}})^2$ . As a result, the particles with  $\epsilon \simeq -\Phi$  (which corresponds to  $r = \mathfrak{R}$ ) dominate in the initial energy spectrum even in the case of quite a steep profile ( $\delta\rho \propto r^{-1}$ ). A strong departure from (6) will take place only if the initial profile is very steep (for instance,  $\delta\rho \propto r^{-3}$ ). On the other hand, such profiles are hardly suitable to describe the initial perturbations of dark matter.

So for a large variety of initial conditions the initial energy distribution of the particles is similar to (6), at least, in the following sense: the majority of the particles have the energy close to  $-\Phi$ , and their energy distribution is quite narrow. In case of distribution (6), for instance, for all the particles  $\epsilon \in [-\frac{3}{2}\Phi; -\Phi]$ . This conclusion is also valid for the warm dark matter. Indeed, the smearing of the energy spectrum with respect to the cold dark matter case is of the order of the temperature of dark matter at the moment of the structure collapse. For the structure to be able to collapse, the temperature should be much lower than  $\Phi$ .

In view of our principle assumption that the energy distribution of the particles changes moderately with respect to the initial one, the similarity between the initial distributions leads to a similarity of the particle energy spectra of the relaxed halo. But how can the system evolve at all, if the energies of the bulk of the particles remain almost the same? The mechanism is the following: the particles oscillate in the potential well. Initially they oscillate cophasal. Then, even if energies of the particles remain constant, their phases diverge. Typically,

the period sharply depends on  $\epsilon$  for the majority of potential wells. But even if the energies of the particles precisely coincide, their phases can diverge as a result of a small nonsphericalness, perturbations from the nearby structures etc. Finally, the phases of the oscillations are mixed thoroughly, and each phase becomes equiprobable. This is exactly the situation, corresponding to the stationary halo. It is important to underline that the phase mixing goes on continuously, in contrast to the energy exchange, which is effective only during the first short stage of violent relaxation.

Finally, the halo collapse forms a stationary potential well  $\phi(r)$ , where  $\phi$  does not depend on time. Each particle can be characterized by its specific angular momentum  $\mu = |[\vec{v} \times \vec{r}]|$  and maximum radius  $r_0$  from the center the particle can reach. Radius  $r_0$  is one-to-one bound with the specific particle energy by evident relationship  $\epsilon = \phi(r_0) + \mu^2/(2r_0^2)$ . We may consider the halo particle distribution function over  $r_0$ .

$$dm = f(r_0) dr_0 \quad (8)$$

If the energy evolution of the halo is moderate,  $f(r_0)$  has a very peculiar appearance. Indeed, the potential well of the collapsed halo is much deeper than the initial one. An initial perturbation had  $k \equiv |(\phi(R_{vir}) - \phi(0))/(\phi(R_{vir}) - \phi(\infty))| \leq 1$ , as we could see from eqn. 6-7, while a formed galactic halo always has  $k \gg 1$ . For instance, a Navarro-Frenk-White halo has  $k \simeq c_{vir}$  (Navarro et al. 1997; Baushev 2012). Accepting for the Milky Way  $M_{vir} = 10^{12} M_{\odot}$ ,  $R_{vir} = 250$  kpc (Klypin et al. 2002), we obtain  $-\Phi = -\phi(R_{vir}) \simeq (130 \text{ km/s})^2$ . Meanwhile, escape speed near the Solar System undoubtedly exceeds 525 km/s (Carney & Latham 1987) and may in principle be much larger (650 km/s or even higher (Marochnik & Suchkov 1984; Binney & Tremaine 2008)). It means that  $k \geq 10$  for the Milky Way and should be even higher for less massive systems. The specific energies of the particles bound in such a well may in principle lie between  $\epsilon = -\Phi$  ( $r_0 \simeq R_{vir}$ ) and  $\epsilon = -k\Phi \simeq -c_{vir}\Phi$  ( $r_0 = 0$ ). However, if we accept *principle assumption* (3), the real energy range occupied by particles is narrower. Indeed, as we could see, the particles are strongly concentrated towards  $\epsilon = -\Phi$  in any reasonable initial perturbation, and if we consider profile  $\rho \propto (2 - (r/\mathfrak{R})^2)$  as a good approximation of real initial perturbations, we saw that the energies of all the particles fall in  $\epsilon \in [-\Phi; -1.6\Phi]$  (see Fig. 1). If assumption (3) is true, it suggests that the majority of the particles still concentrate near  $\epsilon = -\Phi$ : the energy exchange of the particles during the relaxation is more or less a stochastic process, while the total energy of the system should conserve. Thus the narrowness of the initial energy distribution, the relative smallness of the energy evolution, and the fact that the final potential well is much deeper, than the initial one, together result in crowding of the particle apocentre distances  $r_0$  near  $R_{vir}$ .

However, a much more important for us consequence of assumption (3) is that the halo contains almost not at all particles with energies less than  $\epsilon = -1.6\Phi \times \frac{c_{vir}}{3} \simeq -\frac{c_{vir}}{2}\Phi$ . Radius  $r_0$ , corresponding to  $\epsilon = -\frac{c_{vir}}{2}\Phi$ , depends on the density profile. However, it a fortiori ex-

ceeds<sup>1</sup>  $2\frac{R_{vir}}{c_{vir}}$ , which corresponds to the gravitational field of a point mass  $M_{vir}$ ; for a high-concentrated NFW halo  $\epsilon = -\frac{c_{vir}}{2}\Phi$  corresponds to  $r_0 \simeq 2.5\frac{R_{vir}}{c_{vir}}$ . Since condition (3) states that a halo contains only a few particles with  $\epsilon < -\frac{c_{vir}}{2}\Phi$ , it means that the halo contains only a few particles with  $r_0 \in [0; 2\frac{R_{vir}}{c_{vir}}]$ . Actually, a number of particles with  $r_0 \sim 2\frac{R_{vir}}{c_{vir}}$  should also be relatively small, since initial distribution  $\rho \propto (2 - (r/\mathfrak{R})^2)$  contains only a few particles with  $\epsilon \simeq -1.6\Phi$ . We may conclude that distribution function  $f(r_0)$  has a steep maximum near  $r_0 \sim R_{vir}$  and that it is almost equal to zero when  $r_0 \sim (2 - 3)\frac{R_{vir}}{c_{vir}}$ .

The later property is the most important for us. Though the fraction of particles with  $r_0 \leq (2 - 3)\frac{R_{vir}}{c_{vir}}$  is small, the region  $r \leq (2 - 3)\frac{R_{vir}}{c_{vir}}$  is quite large (40-50 kpc for our Galaxy) and contains a very significant fraction of the galaxy mass. It means that the dominant contribution into the dark matter profile in the halo center is given by particles that come there from the outside, i.e. that have apocenter distances  $r_0$  significantly larger than the radius of the region under discussion. Hereafter we will consider even smaller area around the halo center,  $r \leq \frac{R_{vir}}{c_{vir}}$ , where we thus have  $r \ll r_0$  for almost all the particles. On the other hand, this area is still quite large ( $\frac{R_{vir}}{c_{vir}} \simeq 20$  kpc for the Milky Way galaxy). Moreover,  $r = \frac{R_{vir}}{c_{vir}}$  corresponds to the radius where a NFW halo has  $\frac{d \log \rho(r)}{d \log r} = -2$ ; consequently, we may expect that if a halo has a core, its radius is smaller than the radius of the area under consideration.

As we will see, if the central profile is created by particles with  $r \ll r_0$ , the dark matter density profile is quite universal, does not depend on the detailed properties of distribution  $f(r_0)$  and is close to the Einasto profile with  $n \simeq 0.5$ .

### 3. CALCULATIONS

We can easily find the density distribution in the center of the halo, created by the particles coming to this region from the outside, using the method offered in (Baushev 2013a). Let us single out the particles with a certain  $r_0$ . We denote their total mass by  $m$ . N-body simulations (Hansen et al. 2006; Kuhlen et al. 2010) suggest that the distribution over tangential velocities is close, but do not coincide with Gaussian. According to these results, we assume for simplicity that specific angular momentum  $\mu \equiv [\vec{v} \times \vec{r}]$  of the particles has Gaussian distribution

$$dm = m \frac{2\mu}{\alpha^2} \exp\left(-\frac{\mu^2}{\alpha^2}\right) d\mu \quad (9)$$

<sup>1</sup> Here we neglect the part of the particle energy associated with the angular momentum  $\frac{\mu^2}{2r^2}$ . N-body simulations show that the orbits of the majority of the particles are rather prolate (Diemand & Kuhlen 2008), and in this case the influence of the angular momentum on  $r_0$  is negligible. However, even in the worse case of circular orbit,  $r_0$  of a particle cannot be more than two times smaller than one for a radially moving particle with the same energy.

Here  $\alpha \equiv \alpha(r_0)$  is the width of the distribution; generally speaking,  $\alpha$  is a function of  $r_0$ . As we could see, the majority of the particles have  $r_0 \sim R_{vir}$ , and so only those with small  $\mu$  can penetrate into the area of our interest  $r \sim R_{vir}/c_{vir}$ . So the distribution in the halo center is mainly determined by the behavior of (9) when  $\mu \rightarrow 0$ . Thus our calculation is not very sensitive to the assumption of Gaussian distribution: any other distribution with the same behavior at  $\mu \simeq 0$  would give a similar result.

A particle moving in gravitational field  $\phi(r)$  has two integrals of motion:  $\mu$  and  $\epsilon = \frac{v_r^2}{2} + \frac{\mu^2}{2r^2} + \phi$ . The radial velocity of the particle is equal to

$$v_r = \sqrt{2(\phi(r_0) - \phi(r)) - \mu^2 \left(\frac{1}{r^2} - \frac{1}{r_0^2}\right)} \quad (10)$$

We introduce the maximum angular momentum of a particle wherewith it can reach radius  $r$

$$\mu_{max}^2 = 2(\phi(r_0) - \phi(r)) \left(\frac{1}{r^2} - \frac{1}{r_0^2}\right)^{-1} \quad (11)$$

Then (10) may be rewritten as

$$v_r = \frac{\sqrt{r_0^2 - r^2}}{rr_0} \sqrt{\mu_{max}^2 - \mu^2} \quad (12)$$

A particle having maximal radius  $r_0$  and minimal radius  $r_{min}$  contributes into the halo density on all the interval  $[r_{min}, r_0]$ . The contribution of a single particle of mass  $m$  on an interval  $dr$  is proportional to the time the particle passes on this interval (Baushev 2011).

$$\frac{dm}{m} = \frac{dt}{T} = \frac{dr}{v_r T} \quad (13)$$

Here  $T$  is the half-period of the particle, i.e. the time it takes for the particle to fall from its maximal radius to the minimal one

$$T(r_0, \mu) = \int_{r_{min}}^{r_0} \frac{dr}{v_r} \quad (14)$$

$T(r_0, \mu)$  is, generally speaking, a function of  $r_0$  and  $\mu$ .

We can obtain the density distribution from (13), substituting there (12) instead of  $v_r$  and  $4\pi r^2 \rho$  instead of  $dm$ :

$$\rho = \frac{m}{4\pi r^2 v_r T} = \frac{mr_0}{4\pi r T \sqrt{r_0^2 - r^2} \sqrt{\mu_{max}^2 - \mu^2}} \quad (15)$$

In order to find the density distribution produced by all the particles of the halo with a certain  $r_0$ , we should integrate (15) over distribution (9).

$$\rho = \frac{mr_0}{4\pi r \sqrt{r_0^2 - r^2}} \int_0^{\mu_{max}} \frac{2\mu \exp(-\mu^2/\alpha^2)}{\alpha^2 T(r_0, \mu) \sqrt{\mu_{max}^2 - \mu^2}} d\mu \quad (16)$$

This is the exact solution; we can significantly simplify it, however, if we take into account that  $T(r_0, \mu)$  is in general a very weak function of  $\mu$ , especially for small  $\mu$ , since  $T(r_0, \mu)$  has an extremum at  $\mu = 0$ . As we see in Fig. 2,  $T(\mu)$  differs from  $T(0)$  on no more, than 25%, for any reasonable potential, if  $\mu \leq 0.5\mu_{circ}$ , where  $\mu_{circ}$

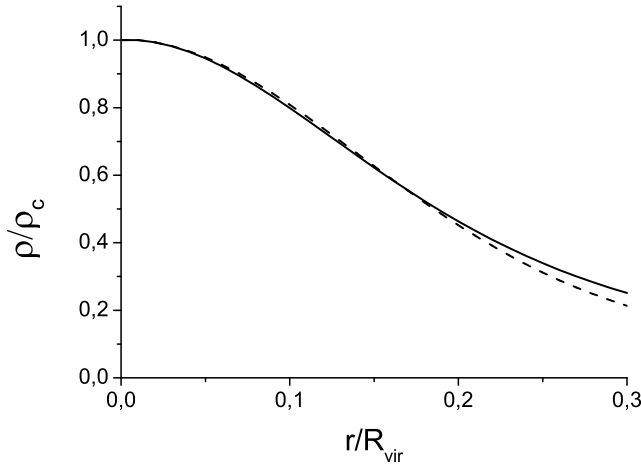


FIG. 3.— The density profile of the exact solution of (16) for  $f(r_0) = M_{vir}\delta(r_0 - R_{vir})$  (dashed line) and profile (21) with the same  $r_c/R_{vir}$  (solid line). One can see that the departure of approximative equation (21) from the exact solution is quite small.

is the angular momentum corresponding to the circular orbit. Only particles with small  $\mu$  can reach the central region under consideration: consequently, we may approximate  $T$  by  $T(r_0, \mu) \simeq T(r_0) \equiv T(r_0, 0)$ : Then we can take the integral in (16)

$$\rho = \frac{mr_0}{2\pi\alpha T(r_0)r\sqrt{r_0^2 - r^2}} D\left(\frac{\mu_{max}}{\alpha}\right) \quad (17)$$

where  $D$  is the Dawson function  $D(x) \equiv e^{-x^2} \int_0^x e^{t^2} dt$ . Of course, all particles in a real halo have some distribution over  $r_0$ :  $dm = f(r_0)dr_0$ . In order to take it into account, we should substitute  $f(r_0)dr_0$  instead of  $m$  to (17) and integrate the result over  $r_0$ . Moreover, equation (17) can be significantly simplified in the central part of the halo. First of all, gravitational potential of the centre of the halo,  $\phi(0)$ , is finite for any reasonable halo profile (otherwise the annihilation signal, produced by the halo, would be infinite, being proportional to  $\int 4\pi r^2 \rho^2 dr$ ). Then we may rewrite (11) as

$$\mu_{max}^2 = 2r^2(\phi(r_0) - \phi(0)) \left(1 - \frac{\phi(r) - \phi(0)}{\phi(r_0) - \phi(0)}\right) \frac{r_0^2}{r_0^2 - r^2} \quad (18)$$

The two last factors may be neglected in the center of the halo, and we can use approximations  $\mu_{max} \simeq r\sqrt{2(\phi(r_0) - \phi(0))}$ ,  $\sqrt{r_0^2 - r^2} \simeq r_0$ . So the total density distribution in the central part is

$$\rho = \int_0^\infty \frac{f(r_0)}{2\pi\alpha(r_0)T(r_0)r} D\left(r\frac{\sqrt{2(\phi(r_0) - \phi(0))}}{\alpha(r_0)}\right) dr_0 \quad (19)$$

We can simplify this equation with the help of the following reasoning. As we could see,  $f(r_0)$  is almost equal to zero for small  $r_0$ . Moreover, the formed halo is dominated by the particles with  $r_0 \sim R_{vir}$ . It means that the main contribution to the integral in (19) is given by the part, where  $r_0 \simeq R_{vir}$ , roughly speaking, by  $r_0 \in [R_{vir}/2; R_{vir}]$ . As we could see, function  $f(r_0)$  sharply depends on  $r_0$  at this interval. On the contrary,  $\alpha(r_0)$  should not change much on interval  $[R_{vir}/2; R_{vir}]$ :  $\alpha(r_0)$  is widely believed to be a power-law dependence with the index between  $-1$  and  $1$  (Hansen et al.

2006).  $\sqrt{2(\phi(r_0) - \phi(0))}$  changes even slower: for instance,  $\sqrt{(\phi(R_{vir}) - \phi(0))/(\phi(R_{vir}/2) - \phi(0))} \simeq 1.1$  for the NFW profile with  $c_{vir} = 15$ . Moreover,  $D$  is a finite and not very sharp function if its argument. Comparing this with the sharp behavior of  $f(r_0)$ , we may neglect the weak dependence of the argument of function  $D$  in (19) on  $r_0$  and substitute there some value, averaged over the halo

$$r_c = \left\langle \frac{\alpha(r_0)}{\sqrt{2(\phi(r_0) - \phi(0))}} \right\rangle \simeq \frac{\langle \alpha(r_0) \rangle}{\sqrt{2|\phi(0)|}} \quad (20)$$

Then we can rewrite (19) and obtain the final result:

$$\rho = \rho_c \frac{r_c}{r} D\left(\frac{r}{r_c}\right), \quad \rho_c = \frac{1}{2\pi r_c} \int_0^\infty \frac{f(r_0)dr_0}{\alpha(r_0)T(r_0)} \quad (21)$$

Since  $D(r/r_c) \simeq r/r_c$ , when  $r/r_c \rightarrow 0$ ,  $\rho_c$  is the central density of the halo. As we can see, it is always finite. At the same time, the shape of the density profile depends on the only parameter  $r_c$ .  $r_c$  defines the radius at which rather a shallow central region of the density profile transforms into a much steeper outer part. So is actually the core radius of profile (21).

In deriving (21), we used several times the fact that  $r \ll r_0$ . This raises the question: for what  $r/R_{vir}$  is equation (21) still valid? In order to check this, we solved numerically exact equation (16) on condition (9) and for distribution  $f(r_0) = M_{vir}\delta(r_0 - R_{vir})$ . Since our approximation  $T(r_0, \mu) \simeq T(r_0, 0)$  is the least acceptable for the particles with high angular momentum, we used the maximal possible value for  $\langle \alpha \rangle = \frac{1}{4}R_{vir}\sqrt{\frac{GM_{vir}}{R_{vir}}} = \frac{1}{4}\sqrt{GM_{vir}R_{vir}}$ . It is apparent that  $\langle \alpha \rangle$  cannot substantially exceed this estimation: otherwise a significant part of the dark matter would not be gravitationally bound in the halo.  $\phi(r)$  appears in expression (16), and we need to write out equation

$$\frac{d\phi}{dr} = \frac{G}{r^2} \int_0^r 4\pi x^2 \rho(x) dx$$

in order to close the task. The exact density profile (dashed line) and profile (21) with the same  $r_c/R_{vir}$  (solid line) are represented in Fig. 3. We see that (21) well approximates the exact solution up to  $r \simeq 0.3R_{vir}$ . So (21) can be valid in quite a large area around the halo centre.

#### 4. DISCUSSION

Fig. 4 represents density profile (21) for  $r_c = R_{vir}/20$ . For comparison, Einasto profile with  $n = 0.5$  and  $r_s = 0.017R_{vir}$  is also plotted. As we can see, the profiles are quite similar, i.e. (21) has a core and is close to Einasto profile with  $n = 0.5$ , which, in its turn, well fits observational dark matter profiles of numerous galaxies (Chemin et al. 2011).

There are two more properties of profile (21) that can be observationally checked. First, Fig. 4 shows that (21) behaves as  $\rho \propto r^{-2}$  at large distances ( $r \gtrsim 1.6r_c$ ). The outer border of the profile (21) applicability is defined by the size of the area where distribution  $f(r_0)$  is almost equal to zero (see the end part of section 2), i.e.,  $r \simeq 2R_{vir}/c_{vir}$ . Since  $1.6r_c$  can be significantly smaller for real galaxies, we may expect a large area

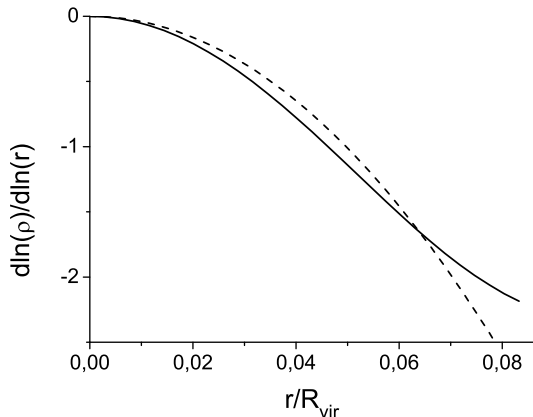


FIG. 4.— Density profile (21) of the central region of a halo with  $r_c = R_{vir}/20$ . Einasto profile with  $n = 0.5$  and  $r_s = 0.017R_{vir}$  is plotted for comparison (dashed line).

with  $\rho \propto r^{-2}$  in the density profile between  $r \gtrsim 1.6r_c$  and  $r \simeq 2R_{vir}/c_{vir}$ . This region is really observed in the profiles of many galaxies (Sofue & Rubin 2001). It is the feature that allowed to prove the existence of the dark matter in 1978 (Rubin et al. 1978). Meanwhile, neither NFW nor Einasto profile has an explicit region with  $\rho \propto r^{-2}$ . Of course, the power index  $\frac{d \log \rho(r)}{d \log r}$  reaches  $-2$  at some radius. This point is nohow separated, however, and there is no reason to expect a large region with the isothermal profile. Though there can be other reasons of its appearance, like the baryon influence, the  $\rho \propto r^{-2}$  profile persistently occurs in many galaxies with very different properties, which implies a fundamental physical mechanism. Profile (21) gives a simple and natural explanation of this effect.

We may roughly estimate the multiplication of the central density  $\rho_c$  on the core radius  $r_c$  (Baushev 2013b). Indeed, if the particles with a certain  $r_0$  have a characteristic velocity  $v$ , then  $\alpha(r_0) \sim r_0 v$ ,  $T(r_0) \sim \tau_d = r_0/v$ , and  $\alpha(r_0)T(r_0) \sim r_0^2$ . Substituting this value into (21), we obtain

$$\rho_c r_c \propto \int_0^\infty \frac{f(r_0)}{r_0^2} dr_0 \quad (22)$$

Now we can follow the same reasoning that we used to transform (19) into (20):  $f(r_0)$  is nonvanishing at  $r \in [2R_{vir}/c_{vir}, R_{vir}]$ . At this interval  $r_0^2$  varies much slower than  $f(r_0)$ , and we may substitute it by some value  $\langle r_0^2 \rangle$  averaged over the halo. Then

$$\rho_c r_c \propto \frac{\int_0^\infty f(r_0) dr_0}{\langle r_0^2 \rangle} = \frac{M_{vir}}{\langle r_0^2 \rangle} \quad (23)$$

As we could see, the majority of the particles have  $r_0 \sim R_{vir}$ , and it is reasonable to assume that  $\langle r_0^2 \rangle \propto R_{vir}^2$ . So  $\rho_c r_c \propto M_{vir}/R_{vir}^2$ . It is more convenient to use the average halo density  $\varrho$ :  $M_{vir} = \frac{4}{3}\pi R_{vir}^3 \varrho$ . We obtain

$$\rho_c r_c \propto M_{vir}^{1/3} \varrho^{2/3} \quad (24)$$

Thus our model predicts that the multiplication of the central halo density on the core radius should be nearly constant for galaxies. Indeed, let us consider the haloes of masses  $10^8 M_\odot$  and  $10^{12} M_\odot$ , which covers almost all

the range of galaxy masses. We denote the quantities related to  $10^8 M_\odot$  and  $10^{12} M_\odot$  haloes by subindexes 8 and 12, respectively.  $M_{vir}^{1/3}$  increases only  $\simeq 20$  times over all the mass interval under consideration. Moreover, the second multiplier  $\varrho^{2/3}$  decreases with  $M_{vir}$ , since less massive galaxies formed earlier, when the universe density was higher. So the multiplier variations partially compensate each other. Virial halo density  $\varrho$  and  $M_{vir}$  are not one-to-one related. The structures appeared from a Gaussian random field, and objects of the same  $M_{vir}$  may have different  $\varrho$ . However, presuming that galaxies with  $10^8 M_\odot$  and  $10^{12} M_\odot$  were formed at  $z_8 = 10$  and  $z_{12} = 4$ , respectively, we may assume that their density ratio is roughly equal to  $\frac{\varrho_8}{\varrho_{12}} \simeq \left(\frac{z_8+1}{z_{12}+1}\right)^3 \simeq 8$  (Gorbunov & Rubakov 2011). Thus our model predicts (24) that  $\rho_c r_c \propto M_{vir}^{1/3} \varrho^{2/3}$  changes only 5 times, when  $M_{vir}$  runs over all the range of the galaxy masses. This prediction is also strongly supported by observations. Kormendy & Freeman (2004) first discovered the constancy of the multiplication of the central halo density on the core radius, and then it was confirmed by several independent observations (see Donato et al. (2009) and references therein). The observations suggest that  $\log(\rho_c r_c) = 1.88 \pm 0.2$  in units of  $\log(M_\odot \text{pc}^{-2})$  for thousands of galaxies with various physical properties.

Thus the supposition of the moderate energy evolution along offers an explanation of three observational properties of galactic haloes. The profile (21) is in agreement with observational data for, at least, some types of galaxies, but clearly disagrees with N-body simulations and observational data for galaxy clusters (Okabe et al. 2010). It suggests that the violent relaxation takes place in galaxy clusters but does not occur in galaxies. There can be various plausible explanations for it: baryon influence, warmth of the dark matter etc. However, the cause may be much simpler: galaxy clusters have low concentrations  $c_{vir} = 3 - 5$ . Condition (3) is very strict for an object with  $c_{vir} = 4$  (the energy of the majority of the particles should not change on more than 30%) and unsatisfiable for  $c_{vir} < 3$ . Galaxies have significantly higher  $c_{vir}$ :  $c_{vir} = 15 - 20$  for massive galaxies and probably even higher for dwarf objects. So in order to be violent, the relaxation should change the energies of a significant part of the particles on 30 - 50% in the case of galaxy clusters and at least five times in the case of galaxies. Consequently, the relaxation may be violent enough to form cusps in galaxy clusters, but moderate in galaxies.

We can now specify the condition of feasibility of our *principle assumption*: a moderate energy evolution of the system during the halo formation. We are interested in the density profile in the very center of the halo ( $r \sim r_c$ , where  $r_c$  is the core radius). We can divide all the particles in this area into two groups:

1. The particles residing this area (with  $r_0 \lesssim r_c$ )
2. The outer particles ( $r_0 \gg r_c$ )

Both the groups give some yield into the density profile of the central region. Our consideration (in particular, the derivation of equation (21)) shows that the contribution of group 2 is always Einasto-like with small Einasto index

( $n \simeq 0.5$ ). So, in order to ascertain that the total density profile of the central part of the halo is close to (21), we only need the contribution of group 1 to be small. This requirement asserts automatically, if the energy exchange between the dark matter particles is moderate in sense (3).

We would like to summarize the main conclusions of this article. First, if the halo relaxation is moderate, the density profile in the central part of a formed halo describes by equation (21), i.e. is Einasto-like with small Einasto index ( $n \simeq 0.5$ ). The profile is quite universal and weakly depends on the shape of the initial perturbation. This is a result of the fact that the potential well of the formed halo is much deeper than that of the initial perturbation. As a result, quite a large area builds up in the centre of the halo, where the particles do not reside, but just come there from the outside: their apoapses lie outside of the area. In order that the orbit of a particle entirely lie within the area, the particle energy should be dramatically decreased with respect to the ini-

tial value. Such a process is always hampered in a dissipationless system, and hence the particles, coming to the central area from the outside, dominate there and form Einasto-like universal density profile (21). The shape of the profile is totally determined by single parameter  $r_c$  (20), which can be considered as the core radius. The model gives a natural explanation for the large areas of nearly isothermal profile  $\rho \propto r^{-2}$  routinely observed in spiral galaxies. Moreover, it predicts the constancy of the multiplication of the central density  $\rho_c$  on the core radius  $r_c$  of dark matter haloes, in good agreement with astronomical data.

Financial support by Bundesministerium für Bildung und Forschung through DESY-PT, grant 05A11IPA, is gratefully acknowledged. BMBF assumes no responsibility for the contents of this publication. We acknowledge support by the Helmholtz Alliance for Astroparticle Physics HAP funded by the Initiative and Networking Fund of the Helmholtz Association.

#### REFERENCES

- Baushev, A. N. 2011, *MNRAS*, 417, L83  
 Baushev, A. N. 2012, *MNRAS*, 420, 590  
 Baushev, A. N. 2013a, *ApJ*, 771, 117  
 Baushev, A. N. 2013b, arXiv:1309.5162, accepted to *A&A*  
 Baushev, A. N. 2013c, arXiv:1312.0314  
 Binney, J. & Tremaine, S. 2008, *Galactic Dynamics: Second Edition* (Princeton University Press)  
 Carney, B. W. & Latham, D. W. 1987, in *IAU Symposium*, Vol. 117, *Dark matter in the universe*, ed. J. Kormendy & G. R. Knapp, 39–48  
 Chemin, L., de Blok, W. J. G., & Mamon, G. A. 2011, *AJ*, 142, 109  
 de Blok, W. J. G. & Bosma, A. 2002, *A&A*, 385, 816  
 de Blok, W. J. G., McGaugh, S. S., & Rubin, V. C. 2001, *AJ*, 122, 2396  
 Diemand, J. & Kuhlen, M. 2008, *ApJ*, 680, L25  
 Diemand, J., Kuhlen, M., & Madau, P. 2007, *ApJ*, 667, 859  
 Diemand, J., Kuhlen, M., Madau, P., Zemp, M., Moore, B., Potter, D., & Stadel, J. 2008, *Nature*, 454, 735  
 Diemand, J., Madau, P., & Moore, B. 2005, *MNRAS*, 364, 367  
 Donato, F., Gentile, G., Salucci, P., Frigerio Martins, C., Wilkinson, M. I., Gilmore, G., Grebel, E. K., Koch, A., & Wyse, R. 2009, *MNRAS*, 397, 1169  
 Einasto, J. 1965, *Trudy Inst. Astroz. Alma-Ata*, 51, 87  
 Evans, N. W. & Collett, J. L. 1997, *ApJ*, 480, L103  
 Gao, L., Navarro, J. F., Cole, S., Frenk, C. S., White, S. D. M., Springel, V., Jenkins, A., & Neto, A. F. 2008, *MNRAS*, 387, 536  
 Garrison-Kimmel, S., Rocha, M., Boylan-Kolchin, M., Bullock, J. S., & Lally, J. 2013, *MNRAS*, 433, 3539  
 Gentile, G., Salucci, P., Klein, U., & Granato, G. L. 2007, *MNRAS*, 375, 199  
 Gorbunov, D. S. & Rubakov, V. A. 2011, *Introduction to the theory of the early universe*  
 Governato, F., Zolotov, A., Pontzen, A., Christensen, C., Oh, S. H., Brooks, A. M., Quinn, T., Shen, S., & Wadsley, J. 2012, *MNRAS*, 422, 1231  
 Hansen, S. H., Moore, B., Zemp, M., & Stadel, J. 2006, *JCAP*, 1, 14  
 Hayashi, E., Navarro, J. F., Taylor, J. E., Stadel, J., & Quinn, T. 2003, *ApJ*, 584, 541  
 Jaffe, W. 1983, *MNRAS*, 202, 995  
 Klypin, A., Prada, F., Yepes, G., Hess, S., & Gottlober, S. 2013, *ArXiv e-prints*  
 Klypin, A., Zhao, H., & Somerville, R. S. 2002, *ApJ*, 573, 597  
 Kormendy, J. & Freeman, K. C. 2004, in *IAU Symposium*, Vol. 220, *Dark Matter in Galaxies*, ed. S. Ryder, D. Pisano, M. Walker, & K. Freeman, 377  
 Kuhlen, M., Weiner, N., Diemand, J., Madau, P., Moore, B., Potter, D., Stadel, J., & Zemp, M. 2010, *JCAP*, 2, 30  
 Landau, L. D. & Lifshitz, E. M. 1980, *Statistical physics*. Pt.1, Pt.2  
 Lynden-Bell, D. 1967, *MNRAS*, 136, 101  
 Marchesini, D., D’Onghia, E., Chincarini, G., Firmani, C., Conconi, P., Molinari, E., & Zacchei, A. 2002, *ApJ*, 575, 801  
 Marochnik, L. S. & Suchkov, A. A. 1984, *The Galaxy*  
 Moore, B., Lake, G., & Katz, N. 1998, *ApJ*, 495, 139  
 Navarro, J. F., Frenk, C. S., & White, S. D. M. 1997, *ApJ*, 490, 493  
 Navarro, J. F., Ludlow, A., Springel, V., Wang, J., Vogelsberger, M., White, S. D. M., Jenkins, A., Frenk, C. S., & Helmi, A. 2010, *MNRAS*, 402, 21  
 Oh, S.-H., de Blok, W. J. G., Brinks, E., Walter, F., & Kennicutt, Jr., R. C. 2011, *AJ*, 141, 193  
 Okabe, N., Zhang, Y.-Y., Finoguenov, A., Takada, M., Smith, G. P., Umetsu, K., & Futamase, T. 2010, *ApJ*, 721, 875  
 Osipkov, L. P. 1979, *Pisma v Astronomicheskii Zhurnal*, 5, 77  
 Planck Collaboration, Ade, P. A. R., Aghanim, N., Armitage-Caplan, C., Arnaud, M., Ashdown, M., Atrio-Barandela, F., Aumont, J., Baccigalupi, C., Banday, A. J., & et al. 2013, *ArXiv e-prints*  
 Pontzen, A. & Governato, F. 2012, *MNRAS*, 421, 3464  
 —. 2013, *MNRAS*, 430, 121  
 —. 2014, *Nature*, 506, 171  
 Power, C., Navarro, J. F., Jenkins, A., Frenk, C. S., White, S. D. M., Springel, V., Stadel, J., & Quinn, T. 2003, *MNRAS*, 338, 14  
 Quinlan, G. D. 1996, *New Astronomy*, 1, 255  
 Rubin, V. C., Thonnard, N., & Ford, Jr., W. K. 1978, *ApJ*, 225, L107  
 Sofue, Y. & Rubin, V. 2001, *ARA&A*, 39, 137  
 Stadel, J., Potter, D., Moore, B., Diemand, J., Madau, P., Zemp, M., Kuhlen, M., & Quilis, V. 2009, *MNRAS*, 398, L21  
 Stiavelli, M. & Bertin, G. 1987, *MNRAS*, 229, 61  
 Syer, D. & White, S. D. M. 1998, *MNRAS*, 293, 337  
 Tremaine, S., Henon, M., & Lynden-Bell, D. 1986, *MNRAS*, 219, 285  
 Wang, J., Frenk, C. S., Navarro, J. F., Gao, L., & Sawala, T. 2012, *MNRAS*, 424, 2715  
 Weinberg, D. H., Bullock, J. S., Governato, F., Kuzio de Naray, R., & Peter, A. H. G. 2013, *ArXiv e-prints*